A miniature microclimate thermal flow sensor for horticultural applications

Dennis Alveringh*†[a], Daniël G. Bijsterveld*, Tomas E. van den Berg*[b], Henk-Willem Veltkamp*[c], Kevin. M. Batenburg*, Remco. G. P. Sanders*, Joost C. Lötters*‡, and Remco J. Wiegerink*
*MESA+ Institute, University of Twente, Enschede, The Netherlands
†Salland Engineering (Europe) B.V., Zwolle, The Netherlands
‡Bronkhorst High-Tech B.V., Ruurlo, The Netherlands
[a]https://orcid.org/0000-0002-9067-7271
[b]https://orcid.org/0000-0002-7202-4699
[c]https://orcid.org/0000-0002-6044-5891
d.alveringh@utwente.nl

***Abstract*—Closely packed plant canopies have a negative influence on the uniformity of conditioned air and therefore induce physiological disorders inside plant production systems. Real-time leaf-level flow measurements help to improve the microclimate. This application needs a small and low-cost flow sensor for a flow regime up to $1\,\mathrm{m\,s^{-1}}$. The chip that is presented in this paper consists of five suspended heavily p-doped silicon beams with resistors integrated in the tip. A fluid flow along these tips causes a temperature difference between the resistors by convective heat transfer, enabling calorimetric flow sensing. The 4.4 mm by 3.6 mm sensor is realized in a three-mask versatile fabrication process. The sensor shows a range of $1\,\mathrm{m\,s^{-1}}$ to $3\,\mathrm{m\,s^{-1}}$ for air with a maximum sensitivity of $1.8\,\mathrm{mV\,m^{-1}\,s}$ and a standard deviation-based accuracy of $3.6\,\mathrm{cm\,s^{-1}}$. The sensor design is easily scalable in theory, hence, a redesign will be made with a slightly lower flow range to fully meet the requirements for the application.**

***Index Terms*—Flow sensor, calorimetric, thermal, microfluidics, horticulture, agriculture, MEMS, microclimate.**

I. Introduction

The increasing world population, the limited availability of agricultural land, and the deficit in yield increase, combined with the effects of climate change, fresh water scarcity, pesticide resistance, and soil degradation challenge world food security [1]–[3]. Greenhouse horticulture and vertical farms[1] can aid in the provision of food to urban populations, where demand is high and long supply chains can lead to food waste [4]. They can deliver high-quality fresh produce that is safe, healthy, tasty, and sustainably produced with high yield and limited land use [4].

Maintaining uniform climate profiles inside these plant production systems remains challenging, due to incomplete air mixing [4]. Closely packed plant canopies hinder the delivery of conditioned air to all the leaves. Areas with stagnant air create a large leaf boundary layer that reduces gas exchange between leaves and the environment [5]. The resulting high relative humidity and temperature reduce plant growth and cause physiological disorders [6], [7].

Airflow patterns can be studied *in silico* with computational fluid dynamics assisting in the determination of an optimal design for the airflow distribution system [8]. However, modeled airflows are often showing large deviations from measurements [9] and the continuously changing plant canopy make modeling complex. Climate control systems with detailed information on the canopy microclimate would therefore be vital to optimize growth in plant production systems because they provide direct information about incomplete air mixing. Ventilation contributes to approximately 8 % of the electrical energy of a plant production system [10], so in addition to increased production efficiency, cost and demand on the power grid could also be reduced.

To meet the application requirements of studying the airflow close to plant leaves, a suitable flow sensor should be sensitive for an airflow in the range of $0\,\mathrm{m\,s^{-1}}$ to $1\,\mathrm{m\,s^{-1}}$ [8], [11]. Preferably, the flow sensor should also be able to measure the direction of the flow. In a recent review paper, several flow sensor principles have been compared [12] including thermal flow sensors, skin friction sensors, and drag force sensors. All sensor principles are capable of measuring in the required flow range. However, since skin friction sensors have a large size [13] and drag force sensors have moving parts that are fragile and vulnerable to pollution [14], thermal flow sensors are preferred, since they are very sensitive to low flow rates [15], have no moving parts [14], are relatively simple to fabricate [14] and operate [15] and are capable of measuring the direction of the flow [16].

To gain more knowledge on airflows in plant production systems we propose a dense network of cheap, accurate and small thermal flow sensors. The small size enables measurements in and around the plant canopy without interference with daily operation. The robust silicon device enables cost-effective production in large volumes. Here we present such a device designed towards the flow regime in the plant production system.

[1]Vertical farms: multilayer indoor plant production system in which all growth factors are precisely controlled to produce high quantities of high-quality fresh produce year round, completely independent of solar light and other outdoor conditions.

2022 IEEE Sensors | 978-1-6654-8464-0/22/$31.00 ©2022 IEEE | DOI: 10.1109/SENSORS52175.2022.9967348

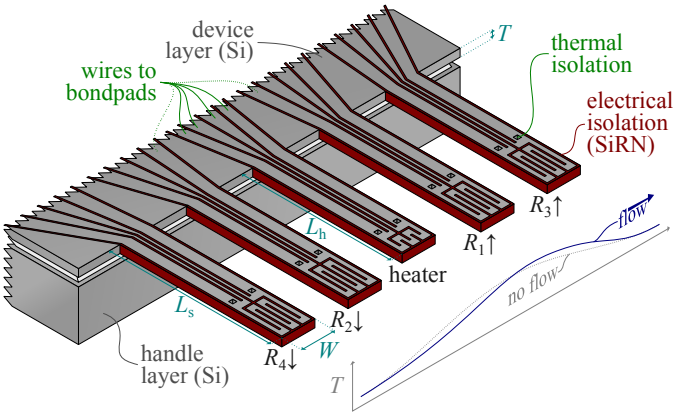

Fig. 1. Illustration of the calorimetric flow sensor consisting of resistors integrated in the tips of five beams. Since all resistors are temperature dependent, an applied flow would increase the resistances R_1 and R_3 and decrease R_2 and R_4. Note that the resistors are integrated in the silicon device layer itself.

II. Design

The chip consists of five beams with resistors integrated in the tip. The central beam is shorter and its resistance is designed to be significantly lower compared to the other beams as can be derived from the dimensions in Table I. The resistor in the tip of the central beam is designed to be used as a heater by applying an electrical current. The resistors of the four other beams are designed to be used as temperature sensors, as the highly p-doped silicon has a positive temperature coefficient of resistance in the required temperature range [17]. A fluid flow along these tips would cool down the resistors upstream and heat up the resistors downstream by convective heat transfer, enabling calorimetric flow sensing. Fig. 1 shows an illustration of the five beams and how these can be used for measuring flow.

TABLE I
Designed dimensions of the structures as indicated in Fig. 1.

	Heater		Sensor	
Length	L_h	502 µm	L_s	552 µm
Width	W	83 µm	W	83 µm
Thickness	T	25 µm	T	25 µm
Resistor length	$L_{h,r}$	0.6 mm	$L_{s,r}$	1.8 mm
Resistor width	$W_{h,r}$	7 µm	$W_{h,s}$	5 µm

III. Experimental setup

The versatile fabrication process is identical to the process presented in [18] and is illustrated in Fig. 2. High aspect ratio trenches are etched in the device layer of a silicon-on-insulator wafer. These trenches are filled with low-stress silicon rich silicon nitride to form electrical isolation. Then, the device and handle layer are etched to form the beams. The final isotropic etching step removes partly the buried silicon oxide layer and releases the chips from the rest of the wafer. In the same step, the large silicon parts between the beams are removed.

The chip measures 4.4 mm by 3.6 mm and is adhesivily bonded to a custom-designed printed circuit board. Electrical

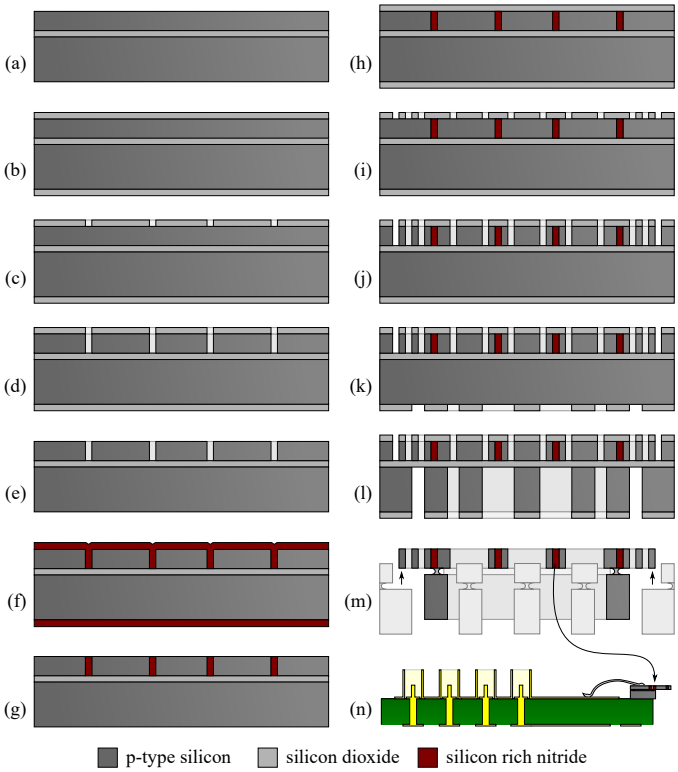

Fig. 2. Illustrations of the fabrication steps, identical to [18]. Fabrication consists of three high aspect ratio plasma etches, a silicon rich silicon nitride deposition step, and one isotropic release etch to release the chips from the rest of the wafer.

connections are made by wirebonding of aluminium wire. Preliminary measurements showed a resistance for the heater and sensor of respectively 0.3 kΩ and 0.6 kΩ with a drift of approximately $1\,\Omega\,d^{-1}$. The drift is probably caused by the contact resistance of the Si-SiO_2-Al interface (i.e. wirebond on native oxide) which is in series with the sensing resistors [19]. This has been reduced to a neglectable level by a 14 day burn-in at 80 mW. A removable silicon bracket as shown in the photograph of the chip in Fig. 3 has been left in place for protection.

The chip is characterized in a custom-made wind tun-

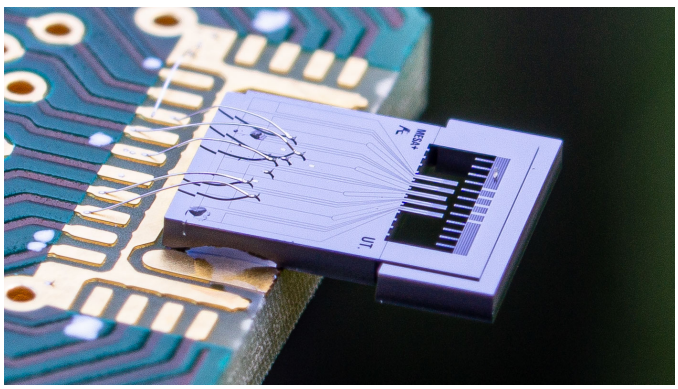

Fig. 3. Photograph of the assembled device. The silicon bracket around the fragile beams can be easily removed, but has been left in place for protection.

nel consisting of a PMMA tube and a 120 mm pulse-width controllable fan (Delta FFC1212DE). The flow in the wind tunnel is measured using a hot-wire anemometer (Voltcraft PL-135HAN). The power in the heater is controlled with a setpoint of 80 mW. The two temperature-sensing beams closest to the heater are the most sensitive for low flows, hence, these are combined with two static resistors in half-Wheatstone bridge configuration. A lock-in amplifier (Stanford Research Systems SR830) is used to apply an alternating supply voltage and detect the magnitude of the bridge voltage. An illustration of the setup is shown in Fig. 4.

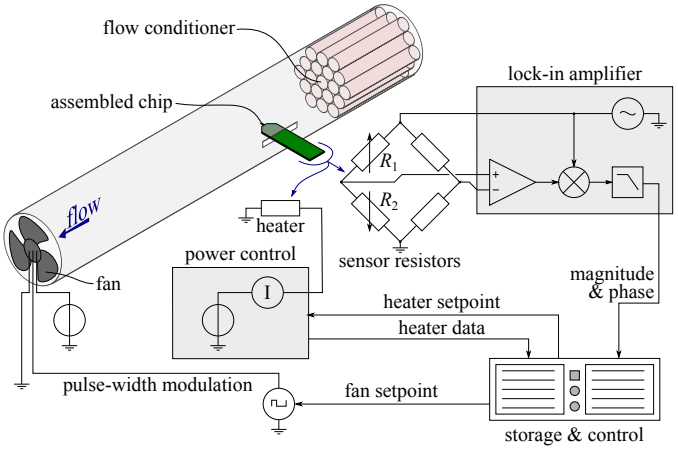

Fig. 4. Illustration of the measurement setup. A laminar flow is applied to the chip using a custom-made wind tunnel. Fan control, heater control and data acquisition are digitally managed by a computer.

IV. Measurement Results

The heater is operated at constant heating power. Fig. 5 shows the measured resistance of the heater and power for different flow velocities. The heater resistance changes approximately 4 %. However, the control loop maintained a heating power within 0.2 mW deviation from the setpoint.

Fig. 6 shows the bridge voltage for different flows. The sensor shows maximum sensitivity of 1.8 mV m^{-1} s (between 1.3 m s^{-1} and 2 m s^{-1}). A standard deviation-based accuracy (100 points) of 6.4 µV translates to an equivalent flow velocity of 3.6 cm s^{-1}.

V. Conclusion

A calorimetric flow sensor with a range of 1 m s^{-1} to 3 m s^{-1} has been designed, fabricated and characterized. The small 4.4 mm by 3.6 mm dimensions of the sensor minimizes the cost-per-die and the influence on the air flow of the sensor itself. The use of highly p-doped single-crystal silicon as heater and sensor material is also expected to be free of drift or material degradation.

The silicon-on-insulator-based fabrication process with silicon-rich silicon nitride isolation has shown high flexibility to realize different types of devices in the same wafer. Therefore, different types and sizes of thermal flow sensors can be fabricated in the future without any recipe changes.

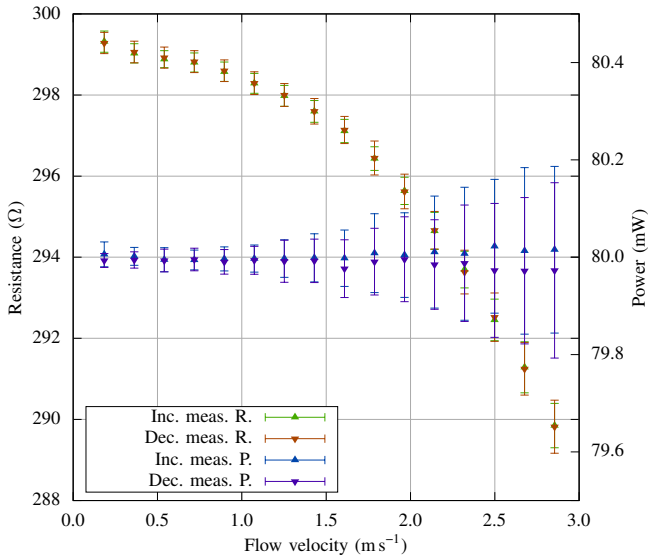

Fig. 5. Measured heater resistance with standard deviation (errorbars), in increasing (▲) and decreasing (▼) order of applied flows and measured (controlled) heater power with standard deviation (errorbars), in increasing (▲) and decreasing (▼) order of applied air flows.

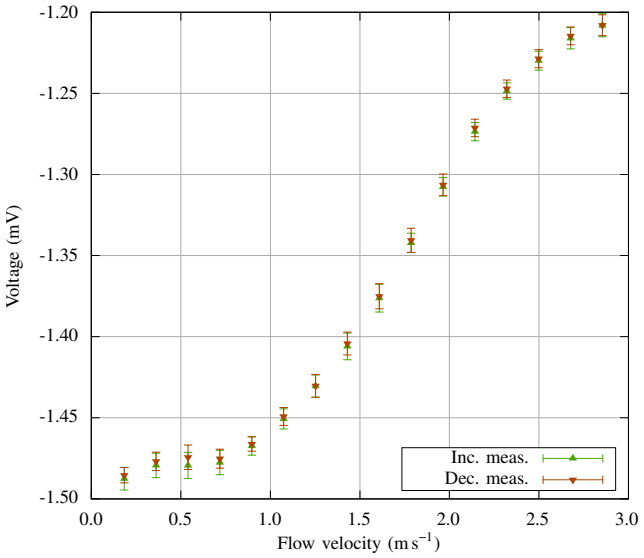

Fig. 6. Measured voltage with standard deviation (errorbars), in increasing (▲) and decreasing (▼) order of applied air flows.

Measuring the air flow at leaf level in plant production systems requires a slightly lower range (i.e., <1 m s^{-1}). However, the sensor design is easily scalable, so future work will focus on the improvement of the sensitivity for low flows by realizing sensors with different gap distances between the sensors and heater. Furthermore, the thermal isolation between sensor tips and the rest of the chip will be improved.

Acknowledgments

The authors gratefully acknowledge the technical support from Erwin Berenschot and the financial support from Sectorplan Bèta and Techniek and the 4TU project Plantenna.

REFERENCES

[1] D. K. Ray, N. D. Mueller, P. C. West, and J. A. Foley, "Yield trends are insufficient to double global crop production by 2050," *PloS one*, vol. 8, no. 6, p. e66428, 2013.

[2] A. J. Challinor, J. Watson, D. B. Lobell, S. Howden, D. Smith, and N. Chhetri, "A meta-analysis of crop yield under climate change and adaptation," *Nature Climate Change*, vol. 4, no. 4, pp. 287–291, 2014.

[3] T. M. Chaloner, S. J. Gurr, and D. P. Bebber, "Plant pathogen infection risk tracks global crop yields under climate change," *Nature Climate Change*, vol. 11, no. 8, pp. 710–715, 2021.

[4] S. van Delden, M. SharathKumar, M. Butturini, L. Graamans, E. Heuvelink, M. Kacira, E. Kaiser, R. Klamer, L. Klerkx, G. Kootstra *et al.*, "Current status and future challenges in implementing and upscaling vertical farming systems," *Nature Food*, vol. 2, no. 12, pp. 944–956, 2021.

[5] T. E. van den Berg, S. Dutta, E. Kaiser, S. Vialet-Chabrand, M. van der Ploeg, T. van Emmerik, M. Coenders-Gerrits, and M.-C. ten Veldhuis, "Plants, vital players in the terrestrial water cycle," in *Instrumentation and Measurement Technologies for Water Cycle Management*, A. S. A. Di Mauro and F. Soldovieri, Eds. Springer Cham, 2022.

[6] B. Aloni, T. Pashkar, and R. Libel, "The possible involvement of gibberellins and calcium in tipburn of Chinese cabbage: study of intact plants and detached leaves," *Plant Growth Regulation*, vol. 4, no. 1, pp. 3–11, 1986.

[7] J. M. Frantz, G. Ritchie, N. N. Cometti, J. Robinson, and B. Bugbee, "Exploring the limits of crop productivity: beyond the limits of tipburn in lettuce," *Journal of the American Society for Horticultural Science*, vol. 129, no. 3, pp. 331–338, 2004.

[8] H. Fang, K. Li, G. Wu, R. Cheng, Y. Zhang, and Q. Yang, "A CFD analysis on improving lettuce canopy airflow distribution in a plant factory considering the crop resistance and LEDs heat dissipation," *Biosystems Engineering*, vol. 200, pp. 1–12, 2020.

[9] T. Boulard, J.-C. Roy, J.-B. Pouillard, H. Fatnassi, and A. Grisey, "Modelling of micrometeorology, canopy transpiration and photosynthesis in a closed greenhouse using computational fluid dynamics," *Biosystems Engineering*, vol. 158, pp. 110–133, 2017.

[10] D. D. Avgoustaki and G. Xydis, "Plant factories in the water-food-energy Nexus era: A systematic bibliographical review," *Food Security*, vol. 12, no. 2, pp. 253–268, 2020.

[11] T. Boulard, H. Fatnassi, J. Roy, J. Lagier, J. Fargues, N. Smits, M. Rougier, and B. Jeannequin, "Effect of greenhouse ventilation on humidity of inside air and in leaf boundary-layer," *Agricultural and Forest Meteorology*, vol. 125, no. 3-4, pp. 225–239, 2004.

[12] F. Ejeian, S. Azadi, A. Razmjou, Y. Orooji, A. Kottapalli, M. E. Warkiani, and M. Asadnia, "Design and applications of MEMS flow sensors: A review," *Sensors and Actuators A: Physical*, vol. 295, pp. 483–502, 2019.

[13] H. Guo, X. Wang, T. Liu, Z. Guo, and Y. Gao, "MEMS skin friction sensor with high response frequency and large measurement range," *Micromachines*, vol. 13, no. 2, p. 234, 2022.

[14] V. Balakrishnan, H.-P. Phan, T. Dinh, D. V. Dao, and N.-T. Nguyen, "Thermal flow sensors for harsh environments," *Sensors*, vol. 17, no. 9, p. 2061, 2017.

[15] P. Bruschi and M. Piotto, "Design issues for low power integrated thermal flow sensors with ultra-wide dynamic range and low insertion loss," *Micromachines*, vol. 3, no. 2, pp. 295–314, 2012.

[16] M. Ahmed, W. Xu, S. Mohamad, F. Boussaid, Y.-K. Lee, and A. Bermak, "Fully integrated bidirectional CMOS-MEMS flow sensor with low power pulse operation," *IEEE Sensors Journal*, vol. 19, no. 9, pp. 3415–3424, 2019.

[17] P. Norton and J. Brandt, "Temperature coefficient of resistance for p- and n-type silicon," *Solid-state electronics*, vol. 21, no. 7, pp. 969–974, 1978.

[18] D. Alveringh, D. L. van der Ven, H.-W. Veltkamp, K. M. Batenburg, R. G. Sanders, D. F. Rivas, and R. J. Wiegerink, "Miniature robust high-bandwidth force sensor with mechanically amplified piezoresistive readout," in *2022 IEEE 35th International Conference on Micro Electro Mechanical Systems Conference (MEMS)*. IEEE, 2022, pp. 684–687.

[19] A. Yu and C. Mead, "Characteristics of aluminum-silicon schottky barrier diode," *Solid-State Electronics*, vol. 13, no. 2, pp. 97–104, 1970.